

Infrared Spectrum of Toluene: Comparison of Anharmonic Isolated-Molecule Calculations and Experiments in Liquid Phase and in a Ne Matrix

Roie Knaanie,[†] Jiří Šebek,^{†,‡} Masashi Tsuge,[§] Nanna Myllys,[§] Leonid Khriachtchev,[§] Markku Räsänen,[§] Brian Albee,^{||} Eric O. Potma,^{||} and R. Benny Gerber^{*,†,§,||}

[†]Institute of Chemistry and The Fritz Haber Research Center, The Hebrew University, Jerusalem 91904, Israel

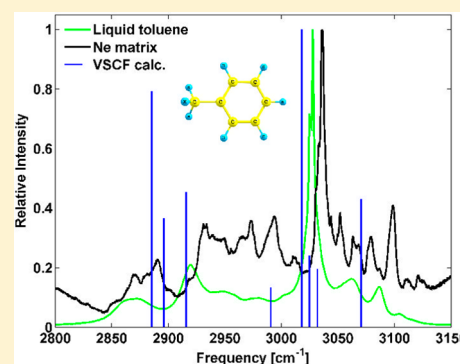
[‡]Department of Physical Chemistry, University of Chemistry and Technology, Prague 16628, Czech Republic

[§]Department of Chemistry, University of Helsinki, P.O. Box 55, FI-00014 Helsinki, Finland

^{||}Department of Chemistry, University of California, Irvine, California 92697, United States

Supporting Information

ABSTRACT: First-principles anharmonic calculations are carried out for the CH stretching vibrations of isolated toluene and compared with the experimental infrared spectra of isotopologues of toluene in a Ne matrix at 3 K and of liquid toluene at room temperature. The calculations use the vibrational self-consistent field method and the B3LYP potential surface. In general, good agreement is found between the calculations and experiments. However, the spectrum of toluene in a Ne matrix is more complicated than that predicted theoretically. This distinction is discussed in terms of matrix-site and resonance effects. Interestingly, the strongest peak in the CH stretching spectrum has similar widths in the liquid phase and in a Ne matrix, despite the very different temperatures. Implications of this observation to the broadening mechanism are discussed. Finally, our results show that the B3LYP potential offers a good description of the anharmonic CH stretching band in toluene, but a proper description of matrix-site and resonance effects remains a challenge.



INTRODUCTION

Vibrational spectroscopy is a fundamental tool for exploring the structure, dynamics, and potential energy surfaces of molecular systems. Among the vibrationally sensitive spectroscopy techniques, infrared (IR) absorption spectroscopy is the method of choice for examining the dipole-allowed vibrational modes in the molecule. However, relating experimental vibrational spectra obtained from IR measurements to actual molecular parameters requires precise calculations. In this work, we combine IR measurements of toluene with accurate anharmonic vibrational calculations.

The main objective of the present paper is to study and interpret the CH stretching band structure of toluene. Our motivation for exploring this molecule is that it is a representative aromatic hydrocarbon with a single CH₃ group. Toluene has a number of CH stretching absorptions in the region between 2800 and 3100 cm⁻¹. Methyl and aromatic CH stretching bands are important for the detection of the hydrocarbon part of organic and biological molecules.¹ Thus, the CH stretching modes have a major role in vibrational spectroscopy of biological molecules; however, assigning the vibrational modes in the CH stretching region is challenging. The CH stretching absorption has a complicated profile formed

by a combination of several overlapping fundamental, overtone, and combination modes, which are difficult to assign.^{1–3}

Previous measurements of the IR vibrational spectrum of liquid toluene at 298 K including assignments and calculations of the integrated intensities were carried out by Bertie et al.,^{4,5} and measurements of IR and Raman spectra of fully deuterated liquid toluene-*d*₈ by Keefe and co-workers.⁶ Reassessments of Bertie's assignments for the vibrational fundamentals were performed by Baker using the scaled quantum mechanical (SQM) force field method.⁷ In an older study, Hitchcock and Laposa measured the IR and Raman spectra of liquid C₆D₅CH₃.⁸

The fluorescence excitation spectrum of the S₁–S₀ transition in jet-cooled toluene has been measured by Selco and Carrick⁹ and Hichman et al.¹⁰ In these studies, the vibrational levels of the S₀ state were determined from dispersed fluorescence spectra. Newer measurements of the CH stretching vibrations of toluene in the S₁ and S₀ states, using IR–UV and UV–IR double resonance spectroscopy in a supersonic jet by

Special Issue: Ronnie Kosloff Festschrift

Received: February 16, 2016

Revised: April 25, 2016

Published: April 26, 2016

Minejima et al.,¹¹ revealed three CH₃ and eight aromatic CH (ring) stretching bands in the S₀ state. It has been suggested that there are anharmonic resonances because the number of experimental bands of the aromatic ring (eight) exceeds the theoretical number (five).

In the present study, spectroscopic measurements of toluene were carried out in two different environments. The first one was liquid toluene measured at room temperature, and the other experiment was made on toluene molecules isolated in a Ne matrix at 3 K. Spectra at such low temperatures often exhibit features that are not observed at room temperature where the broadening effects are stronger. Spectroscopy in low-temperature matrixes provides an opportunity to explore fine features that may be masked at higher temperatures.¹² Toluene isotopologues and their interaction with xenon and N₂O in a Ne matrix have been recently studied by Cao et al.^{13,14} In particular, they have measured and calculated the vibrational spectra of normal toluene, C₆H₅CD₃,¹³ and C₆D₅CH₃¹⁴ and assigned the spectra on the basis of harmonic calculations (including the CH and CD stretching modes).

Quantum chemical calculations are important for interpretation and assignments of spectral bands. The simplest vibrational analysis employs the harmonic approximation.^{15,16} Harmonic calculation is fast and feasible for relatively large organic molecules, but its accuracy is limited,^{17–19} in particular, for stretching vibrations. Hydrogenic stretches of hydrocarbons show large anharmonic shifts,^{3,20} therefore, we need to consider anharmonic vibrational methods. Anharmonic calculations for relatively large molecules are difficult due to the nonseparability of the Hamiltonian.²¹ Several methods for anharmonic spectra calculations are available. Barone^{22,23} implemented a method based on the perturbation correction for the harmonic approximation, which is included in the GAUSSIAN program package.²⁴ Gageot and co-workers^{25–28} have applied the Car–Parrinello classical molecular dynamics simulations.²⁹ There are other approaches available in the literature.^{30–33}

In the present study, we calculate anharmonic vibrational spectra by applying the vibrational self-consistent field (VSCF) approximation and its enhancements,^{16,21} directly using *ab initio* potential surfaces. This method does not require fitting the potential energy surfaces, scaling factors^{34,35} or empirical parameters. The VSCF algorithm is implemented in the electronic structure program GAMESS,³⁶ it is accurate and yet inexpensive computationally. VSCF calculations have been successfully applied for small to medium sized biomolecules.^{2,37,38} The VSCF method is briefly described in the Methodology section.

METHODOLOGY

IR Measurements of Liquid Toluene at Room Temperature. The IR measurements of liquid toluene were carried out using a Nicolet Magna-IR 860 Fourier transform infrared (FTIR) spectrometer. A CaF₂ sealed cell (PerkinElmer) with a path length of 0.025 mm was loaded with toluene (Sigma-Aldrich, 99.9%). An average of 100 FTIR spectra was collected under ambient conditions to improve signal-to-noise. The resolution of the measurements was 1 cm⁻¹.

IR Measurements in Ne Matrixes. Gaseous mixtures of toluene and Ne were made in a vacuum line with a standard manometric procedure with molar ratios toluene/Ne = 1/2000 to 1/10000. Liquid toluene samples, C₆H₅CH₃ (Sigma-Aldrich, 99.8%), C₆D₅CH₃ (Cambridge Isotope Laboratories, 99.8% isotopic purity), C₆H₅CD₃ (Cambridge Isotope Laboratories,

99.8% isotopic purity), and C₆D₅CD₃ (Sigma-Aldrich, ≥ 99% isotopic purity), were degassed by several freeze–pump–thaw cycles. The gaseous mixtures were deposited onto a CsI substrate kept at 3.0 K in a closed-cycle helium cryostat (SHI, RDK-408D2). IR spectra in the 4000–400 cm⁻¹ spectral range with 0.125 cm⁻¹ resolution were measured using a Vertex 80v FTIR spectrometer (Bruker) coadding 500 scans.

Geometry Optimizations and Harmonic Quantum Chemical Calculations. The geometry optimizations and harmonic vibrational calculations were performed by the DFT B3LYP^{39,40} and the second-order Møller–Plesset perturbation theory (MP2) methods.⁴¹ The calculations were performed using the electronic structure program GAMESS.³⁶ We used the correlation consistent polarized valence double- ζ basis set (cc-pVDZ) proposed by Dunning^{42,43} in all calculations. The cc-pVDZ basis is feasible for the VSCF calculations for systems with 10–20 atoms. Its accuracy is sufficient for comparison with experiment.^{2,20,44,45} The quantum chemical, anharmonic Vibrational Self-Consistent Field (VSCF) calculations for an isolated molecule were carried out using GAMESS.

VSCF Methods. Anharmonic interactions including coupling between different modes are calculated using the VSCF method and its extensions.^{16,18,19,46–58} Detailed description of this method can also be found in a recent review by Roy and Gerber.²¹ The VSCF calculations in this study used mass weighted normal coordinates Q_i . For the potential, we used the pairwise approximation, i.e., a sum of single-mode (diagonal) and pair-coupling terms, neglecting higher-order coupling interactions between different normal modes. The potential requires multidimensional grid point calculations. For 16-point grids along each normal coordinate and M vibrational modes, the number of total grid points (GP) is

$$GP = 16 \times M + \frac{[M(M-1) \times 16^2]}{2} \quad (1)$$

for the diagonal and coupling terms. The calculated potentials are then used for the numerical solution of the one-dimensional VSCF equations. A self-consistent field approach is used; i.e., all the equations are solved numerically until the convergence is reached. The anharmonic intensities of the fundamentals and overtones are obtained by the following formula:

$$I_i = \frac{8\pi^3 N_A}{3hc} \omega_i |\langle \Psi_i^{(0)}(Q_i) | \vec{\mu}(Q_i) | \Psi_i^{(m)}(Q_i) \rangle|^2 \quad (2)$$

Here, $\vec{\mu}$ is the dipole moment vector, ω_i is the vibrational frequency of the normal mode i , and $\Psi_i^{(0)}$ and $\Psi_i^{(m)}$ are the VSCF wave functions for the ground and the m th excited vibrational states. For combination transitions involving modes i and j , the IR intensities (I_{ij}) are obtained by

$$I_{ij} = \frac{8\pi^3 N_A}{3hc} \omega_{ij} |\langle \Psi_i^{(0)}(Q_i) \Psi_j^{(0)}(Q_j) | \vec{\mu}(Q_i, Q_j) | \Psi_i^{(m)}(Q_i) \Psi_j^{(n)}(Q_j) \rangle|^2 \quad (3)$$

where m and n are excitation levels for modes i and j .

VSCF-PT2. The VSCF results can be improved using the second order perturbation theory (VSCF-PT2), also referred to as CC-VSCF.^{59,60} This method is analogous to the Møller–Plesset method known in the context of electronic structure calculation.⁴¹ A detailed description of this method and its applications can be found elsewhere.^{61–63} Several different VSCF codes and various improved approaches also exist in the literature.^{64–71}

Simulation of the Line Shape. The spectral line shapes were constructed in our calculations assuming that the transitions have Lorentzian shapes with the full widths at the half-height (fwhh) of 6 cm^{-1} . This value was estimated according to the fwhh of the most intense band in the liquid-toluene spectrum. Note that, for simplicity, our calculation employed a single width for all bands although different experimental bands have different widths. A similar approach was used for other systems, e.g., for some saccharides³⁸ and hydrocarbons.^{3,20} Both the experimental and calculated spectra were normalized to the highest peak.

RESULTS AND DISCUSSION

The VSCF calculations were carried out for four isotopologues of toluene, and the calculated spectra were compared to the experimental spectra in the liquid phase and in a Ne matrix. The comparison between theory and experiments in two environments with large temperature difference enables us to make a better interpretation of the spectra.

IR Spectrum of Liquid Toluene and B3LYP VSCF Calculations. The experimental IR spectrum of liquid toluene and the B3LYP VSCF spectrum are shown in Figure 1. The

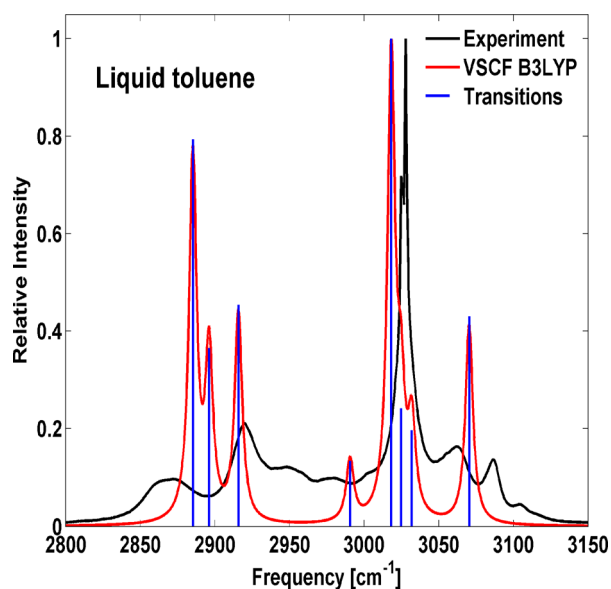


Figure 1. B3LYP VSCF spectrum of toluene (red line) with the VSCF lines corresponding to all fundamental transitions in this spectral range (blue lines), compared to the IR liquid-phase experiment (black line). The B3LYP VSCF spectrum of toluene is obtained as a superposition of Lorentzian bands with the fwhh of 6 cm^{-1} .

calculated vibrational frequencies and intensities for the CH stretching modes at both harmonic and anharmonic levels are presented in Table 1. The fwhh value (6 cm^{-1}) of the calculated spectrum was chosen to reproduce the profile of the highest peak of the experimental spectrum. As mentioned previously, a single parameter was employed across the spectrum although the widths of different bands are different. It can be seen that the overall agreement between the experimental peak positions and the B3LYP VSCF fundamental frequencies is good. Detailed comparison between the B3LYP VSCF calculations and the experiment (Table 1) shows that the average absolute deviation (AAD) between the experimental and B3LYP VSCF frequencies is about 15 cm^{-1} (0.5%), and the root-mean-square deviation (RMSD) is 17.5 cm^{-1} . The

harmonic B3LYP frequencies are less accurate, as expected, with an AAD of 153 cm^{-1} (5.15%) from the experiment. Note that the frequency order for the harmonic and VSCF frequencies is different. The average difference between the relative experimental and B3LYP VSCF intensities (Table 1) is about 50%. The errors of intensities are usually much larger than those of frequencies.²¹ In this study, we mainly analyze the frequencies.

The experiment shows more bands than the calculations. Our assignments for the upper five transitions of the aromatic C_6H_5 ring to the experimental peaks indicate that the calculated transitions are mostly red-shifted compared to the experimental peaks. We suggest that the shift and splitting of the experimental bands in comparison with the calculated transitions is at least partly due to Fermi resonances. This interpretation is supported by comparison between the calculations and Ne-matrix experiments, which will be discussed later.

Comparison of the Spectra from the B3LYP and MP2 Potential Energy Surfaces. The VSCF and VSCF-PT2 IR spectra for the MP2/cc-pVDZ and B3LYP/cc-pVDZ potentials were calculated and compared with the experimental spectrum of liquid toluene in Table 1. Comparison of the four anharmonic spectra to the experiment shows the following frequency order for the CH stretching frequencies: B3LYP VSCF-PT2 < B3LYP VSCF < experiment < MP2 VSCF-PT2 < MP2 VSCF. The B3LYP VSCF and MP2 VSCF-PT2 methods produce the best agreement with the experiment, and on the whole are of comparable performance. Similar conclusions for these potentials have been found in a recent study by Roy et al.⁷² Overestimation of the CH stretching frequencies by the MP2 method has been reported for other hydrocarbons.^{2,3,45} Taking into account both intensity and frequency differences between the calculation and the experiment, we see that the B3LYP VSCF method gives the best results. Furthermore, for nearly degenerated systems like the aromatic CH and CH_3 stretching modes in toluene, the VSCF-PT2 method, which is not adopted for degeneracy, may be less reliable compared to the VSCF method.^{3,21} In this case, we found that the degeneracy problem of VSCF-PT2 did affect the results, at least for some of the transitions, whereas the VSCF calculations exhibit no such problem in all cases. In addition, we notice that the VSCF results are satisfactory in comparison with experimental data. This is also compatible with results on other hydrocarbons.³ On the basis of these reasons, we will use the B3LYP VSCF spectra in the following discussion whereas, for comparison, the VSCF-PT2 results will also be presented. Advanced variants of VSCF theory such as vibrational configuration interaction (VCI) and especially VSCF-VDPT,⁶⁹ which employ the degenerate perturbation theory, are better than the present methods. However, the VCI and VSCF-VDPT calculations are substantially more demanding in this case, whereas the VSCF results are in accord with the experiment.

A higher accuracy can be achieved by more advanced potentials, indeed. For example, in a recent study,⁴⁵ it has been found that a new hybrid MP2/MP4 potential yields a very good agreement with experiment for four selected molecules, better than the B3LYP and MP2 potentials.

Ne Matrix Experiments and B3LYP VSCF Calculations. The Ne matrix spectrum of toluene $\text{C}_6\text{H}_5\text{CH}_3$ in the CH stretching region is compared to the B3LYP VSCF spectrum in Figure 2. In addition to the fundamental transitions, the

Table 1. Harmonic and Anharmonic Vibrational Frequencies (cm^{-1}) of the CH Stretching Modes of Toluene and the Experimental Spectrum of Liquid Toluene

mode ^a	MP2/cc-pVDZ			B3LYP/cc-pVDZ				mode type	exper liquid toluene	
	harm.	VSCF	VSCF-PT2	harm	VSCF	VSCF-PT2	VSCF IR intensity ^b		freq	rel intensity ^c
ν_1	3242	3121	3088	3194	3070	3038	16.7	CH sym	3087	0.14
ν_2	3230	3062	3035	3181	3018	2996	38.8	CH asym	3028	1.00
ν_3	3220	3081	3016	3173	3032	2919	7.61	CH asym	3062	0.16
ν_4	3206	3038	3010	3159	2991	2966	5.19	CH asym	3001	0.10
ν_5	3204	3073	3011	3157	3025	2957	9.36	CH asym	3025	0.72
ν_6	3185	2964	2922	3111	2896	2857	14.2	CH ₃ asym	2920 ^d 2873	0.10
ν_7	3165	2984	2928	3082	2916	2901	17.6	CH ₃ asym	2949 ^d 2920	0.21
ν_8	3077	2952	2929	3021	2885	2890	30.8	CH ₃ sym	2873 ^d 2862	0.09

^aMode numbers are given on the basis of the B3LYP/Harm frequencies. ^bInfrared intensities (km mol^{-1}) are calculated at the B3LYP/VSCF level. ^cRelative peak heights. ^dAssignment uncertain.

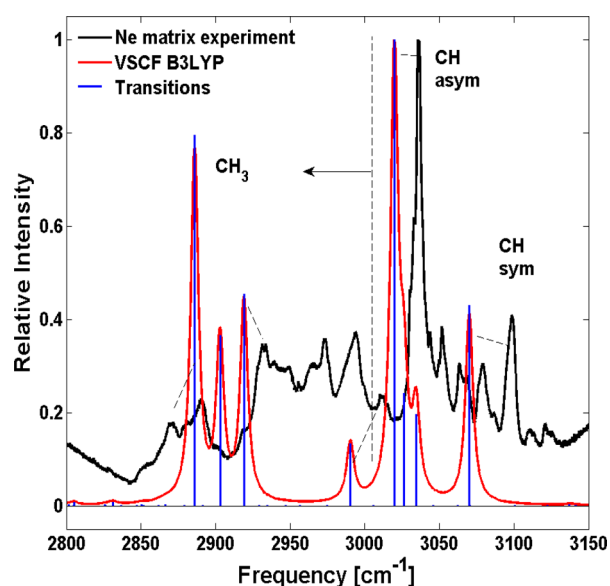


Figure 2. B3LYP VSCF spectrum of toluene $\text{C}_6\text{H}_5\text{CH}_3$ with the combinations and overtones (red line) and the VSCF lines corresponding to all the transitions in this spectral range (blue lines), compared to the Ne matrix experiment (black line).

calculated overtones and combination bands are also shown. Although there are only eight fundamental transitions between 2885 and 3070 cm^{-1} , the Ne matrix spectrum shows at least 12 peaks (Table 2). The experimental spectrum of toluene in a Ne matrix has recently been measured by Cao et al.,¹³ and their results are in good agreement with our experiment. Their frequencies calculated at the MP2/aug-cc-pVTZ level are larger than the experimental ones, similarly to our harmonic MP2 frequencies. We have found that the harmonic MP2 frequencies are less accurate (average deviation of $\sim 6\%$) compared to the B3LYP VSCF ones (average deviation is $< 1\%$). The order of the VSCF and harmonic frequencies is different due to the anharmonic effects, and hence these methods may lead to different assignments of the experimental bands.

The RMSD between the B3LYP VSCF and experimental fundamental frequencies in Table 2 is 18.5 cm^{-1} . The RMSD is 60 cm^{-1} for VSCF-PT2 and 147.3 cm^{-1} for the harmonic calculations, i.e., much larger than for the VSCF method.

Splitting of the bands in the Ne matrix spectrum (Figure 2) is observed both in the aromatic CH stretching region (3015–3120 cm^{-1}) and in the methyl stretching region (2850–3000 cm^{-1}). Similarly to the liquid-phase IR spectrum, the calculated CH stretching bands are mostly red-shifted compared to the experimental positions. The observed shifts and major splitting of the experimental bands in comparison with the calculated transitions may be due to Fermi resonances. The B3LYP VSCF overtones and combination bands near the fundamentals, which can lead to Fermi resonances, are given in Table 2. The calculations for overtones and combinations are not rigorous. Our codes compute the frequencies of overtones and combinations, but they do not include the Fermi resonances. In other words, they cannot predict the significance of Fermi resonance (i.e., the degree of splitting) but they can indicate the possibility of Fermi resonances. The IR–UV double resonance measurements for the CH transitions of jet-cooled toluene in the S_0 state by Minejima et al.¹¹ show similar band splittings and support the involvement of Fermi resonances. Several other mechanisms can lead to the band splitting, such as coupling of the vibrational transitions and rotation of the methyl group. In addition, splitting due to different matrix sites cannot be completely excluded, especially for the fine band structure. The shift can also be due to the limitations in the calculations.

It should be emphasized that the experimental bands presumably originate from monomeric toluene in a Ne matrix because the experiments with different molar ratios of toluene:Ne = 1:2000 and 1:10000 samples give quite similar spectra. In addition, the similarity of the spectrum of toluene in Ne matrixes, the spectrum of jet-cooled toluene,¹¹ and the spectrum of liquid toluene indicates that interpretation in terms of an isolated toluene molecule is reasonable.

Figure 3 shows the spectra of different isotopologues of toluene in Ne matrixes. This comparison confirms the separation of the bands between aromatic CH and methyl stretching bands given in Figure 2. In particular, it clearly shows that the weak 3011 cm^{-1} band belongs to the aromatic CH stretching modes as indicated by an arrow. This assignment is supported by the B3LYP VSCF calculations.

We note that in a Ne matrix at 3 K, there is a substantial effect of broadening. The fwhh is about 6 cm^{-1} , similar to the fwhh of the strongest band in the liquid phase (Figure 4). This may seem surprisingly large, given that the temperature of Ne

Table 2. Harmonic and Anharmonic Vibrational Frequencies (cm^{-1}) of the CH Stretching Modes of Normal Toluene ($\text{C}_6\text{H}_5\text{CH}_3$) Including the Overtones and Combination Bands and the Experimental Spectrum in a Ne Matrix

mode	B3LYP harmonic	B3LYP VSCF	B3LYP VSCF-PT2	VSCF IR intensity [km mol^{-1}]	Ne matrix experiment ^a	assign.
$\nu_7 + \nu_{39}$	3154	3197	3101	0.54		
$\nu_6 + \nu_{39}$	3182	3177	3075	0.52		
$\nu_7 + \nu_{38}$	3296	3137	3102	0.11		
ν_1	3194	3070	3039	16.70	3099 3079 ^b 3064 ^b (3098.2) (3078.4) (3064.8)	CH sym (ring)
ν_3	3173	3034	2939	7.61	3052 (3051.4)	CH asym
ν_5	3157	3026	2959	9.37	3044 ^b	CH asym
ν_2	3181	3020	2999	38.85	3037 (3035.7)	CH asym
ν_4	3159	2990	2967	5.20	3011	CH asym
ν_7	3082	2919	2896	17.66	2993 ^b 2973 ^b 2931 (2993.3) (2970.8)	CH ₃ asym
ν_6	3111	2903	2869	14.22	2931 ^b 2891 ^b (2932.1)	CH ₃ asym
ν_8	3021	2886	2889	30.92	2891 2869 ^b (2890.7)	CH ₃ sym
$2\nu_{13}$	2915	2866	2848	0.12		
$2\nu_{14}$	2899	2850	2847	0.08		
$\nu_{11} + \nu_{17}$	2852	2831	2828	0.28		
$\nu_{10} + \nu_{18}$	2865	2826	2822	0.07		
$\nu_{13} + \nu_{15}$	2856	2805	2799	0.26		
$\nu_9 + \nu_{20}$	2824	2802	2797	0.11		

^aFrequencies in parentheses are from ref 13. ^bAssignment uncertain.

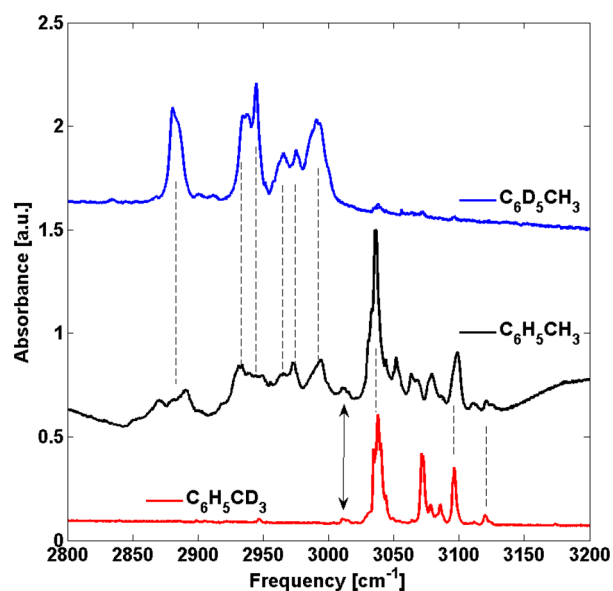


Figure 3. IR spectra of normal toluene $\text{C}_6\text{H}_5\text{CH}_3$ (the middle black line), of partially deuterated toluene $\text{C}_6\text{D}_5\text{CH}_3$ (upper blue line) and $\text{C}_6\text{H}_5\text{CD}_3$ (lower red line) in a Ne matrix.

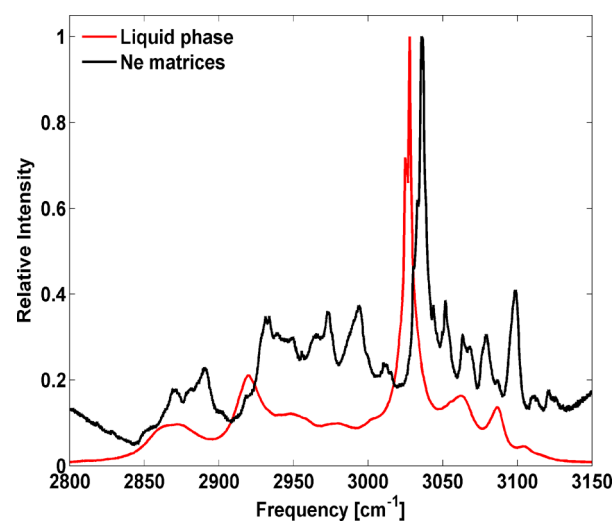


Figure 4. Experimental vibrational spectra of toluene: liquid toluene (red line) and toluene in a Ne matrix (black line).

matrix is 2 orders of magnitude lower than in the liquid. Possible broadening mechanisms are suggested in the concluding discussions. The other peaks in the liquid phase

are much wider than 6 cm^{-1} as well as than the bands in a Ne matrix, especially in the methyl stretching region.

The comparison of the B3LYP VSCF frequencies to the Ne matrix spectrum and to the liquid-phase experiment shows similar shifts between theory and experiment, especially for the strongest peaks. The reasonable success of VSCF with the B3LYP potential for both environments suggests that this method is useful for spectral analysis of similar systems.

Ne Matrix Experiments: Spectra of $\text{C}_6\text{D}_5\text{CH}_3$ Compared to the B3LYP VSCF Calculations. Figure 5 shows the

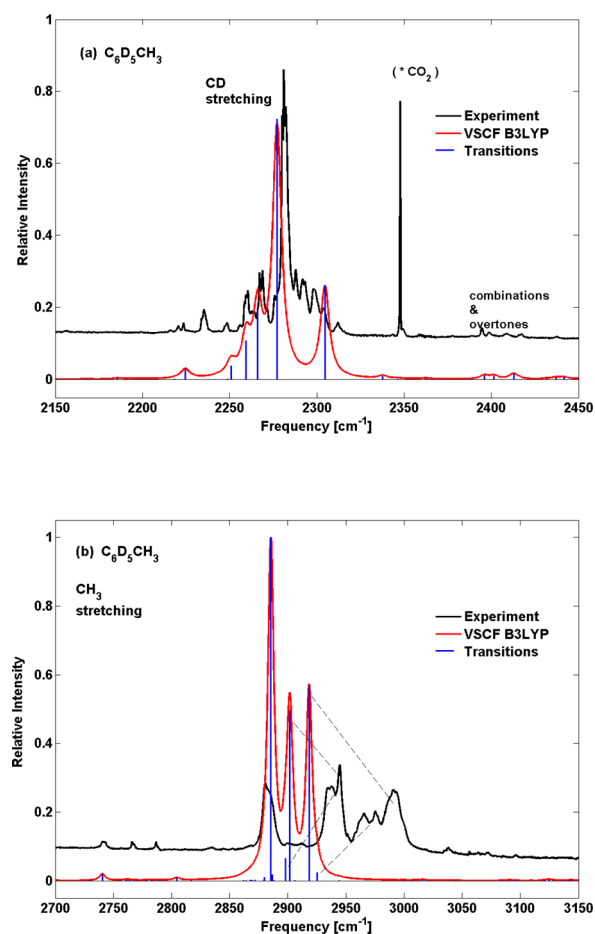


Figure 5. B3LYP VSCF spectra of partially deuterated toluene $\text{C}_6\text{D}_5\text{CH}_3$ with the combinations and overtones (red line) and VSCF lines corresponding to all the transitions in this spectral range (blue lines), compared with the spectrum of $\text{C}_6\text{D}_5\text{CH}_3$ in a Ne matrix (black line). (a) Aromatic CD stretching region. (b) CH_3 stretching region. Dashed lines indicate possible Fermi resonance pairs.

spectrum of partially deuterated toluene $\text{C}_6\text{D}_5\text{CH}_3$ in a Ne matrix and the B3LYP VSCF spectrum. Frequencies and intensities for the overtone and combination modes found near the fundamentals are listed in Table 3, together with the experimental frequencies. The CH_3 stretching frequencies of $\text{C}_6\text{D}_5\text{CH}_3$ in a Ne matrix have been reported by Cao et al.¹⁴ (Table 3); the reported frequencies are slightly different from our values possibly due to different concentration and deposition temperatures. The harmonic spectrum calculated by the M06-2X/aug-cc-pVTZ method shows good agreement with the experiment. The AAD between B3LYP VSCF and experiment for the fundamental transitions, ν_1 – ν_8 , is 0.56%, and the RMSD is 30 cm^{-1} (Table 3). For the aromatic CD

stretching transitions, ν_4 – ν_8 , the VSCF RMSD is only 2.3 cm^{-1} , whereas for the methyl stretching transitions, ν_1 – ν_3 , it is larger (48.9 cm^{-1}). This is perhaps because CD stretches are less anharmonic than CH or CH_3 stretches (D is heavier than H), and also presumably due to Fermi resonances of the methyl bands. The VSCF-PT2 results (RMSD = 47.7 cm^{-1} , AAD = 1.4%), and the harmonic calculations (RMSD = 101.4 cm^{-1} , AAD = 3.7%), are less accurate than the VSCF.

Figure 5a depicts the spectrum in the region of the aromatic CD stretching modes. In a Ne matrix, the experimental spectrum (black line) is split into many peaks, exceeding the five theoretical fundamental transitions. The B3LYP VSCF overtones and combination bands with frequencies close to those of some fundamentals may allow the occurrence of Fermi resonances. Figure 5b shows the CH_3 stretching region. The calculated transitions are red-shifted compared to the experimental spectrum (black line), which is split similarly to the case of normal toluene (Figure 2).

As suggested above, the major splitting in the region of the methyl stretching modes can be due to Fermi resonance. Possible Fermi resonance pairs are indicated by dashed lines in Figure 5b. The calculated IR intensities of the transitions $\nu_4 + 2\nu_{39}$ (predicted at 2925 cm^{-1}), $\nu_5 + 2\nu_{39}$ (2898 cm^{-1}), and $\nu_6 + 2\nu_{39}$ (2887 cm^{-1}), where the ν_{39} mode is methyl torsional rotation mode, are relatively high (Table 3), and their frequencies differ by 7 cm^{-1} or less from the ν_2 (predicted at 2918 cm^{-1}), ν_1 (2902 cm^{-1}), and ν_3 (2885 cm^{-1}) fundamentals, respectively. This may explain the splitting of the three experimental CH_3 stretching bands seen in Figure 5b. The VSCF calculations of the overtone and combination modes included only pairs of the combination modes and only the second order for the overtone modes. There are overtones and combination modes of higher order that may have considerable intensities; however, they are not considered in this work. The coupling with librational modes and rotation of the methyl group are also possible reasons for the observed splitting.

We emphasize again that the experimental bands are relatively broad. The experimental fwhh is about 6 cm^{-1} for the aromatic CD stretching, and even larger for the methyl stretching bands. The broadening mechanism is discussed below.

Ne Matrix Experiments: Spectrum of $\text{C}_6\text{H}_5\text{CD}_3$ Compared to the B3LYP VSCF Calculations. The Ne matrix spectrum of partially deuterated toluene $\text{C}_6\text{H}_5\text{CD}_3$ is compared to the B3LYP VSCF calculations in Figure 6. The CD_3 stretching bands of $\text{C}_6\text{H}_5\text{CD}_3$ were also measured and calculated by Cao et al.¹³ Their measurements are in good agreement with our experiment (Table S1 in the Supporting Information) whereas their harmonic MP2 calculations show a blue shift compared to the experiment and to the present B3LYP VSCF calculations.

Figure 6a shows the aromatic CH stretching region. The experimental CH stretching frequencies of $\text{C}_6\text{H}_5\text{CD}_3$ are similar to those of normal toluene. It justifies the assignments for the aromatic stretching of toluene shown in Figure 2 by dashed lines. The combinations and overtones seem not to contribute in this region. Figure 6b shows the CD_3 stretching region (from 2100 to 2250 cm^{-1}). The calculated transitions are red-shifted compared to the experimental ones. The relatively strong experimental peaks below 2100 cm^{-1} are assigned to the $\nu_9 + 2\nu_{39}$ and the $\nu_{24} + \nu_{25}$ combination modes (experimental peak at 2066 and 2068 cm^{-1}) and the $2\nu_{24}$ overtone (experimental peak at 2087 cm^{-1} ; see also Table S1). The experimental bands

Table 3. Vibrational Frequencies (cm^{-1}) of the Methyl CH and Aromatic CD Stretching Modes of Partially Deuterated Toluene ($\text{C}_6\text{D}_5\text{CH}_3$) at the Harmonic and Anharmonic Levels Including the Overtones and Combination Bands and the Experimental Spectrum in a Ne Matrix

mode	B3LYP harmonic	B3LYP VSCF	B3LYP VSCF-PT2	VSCF IR intensity [km mol^{-1}]	Ne matrix	assign.
$\nu_4 + 2\nu_{39}$	2512 ^c	2925	2902	0.74		
ν_2	3082	2918	2897	17.82	2991 2975 ^a 2965 ^a (2985.1) ^b	CH ₃ asym
ν_1	3111	2902	2868	15.51	2945 2938 ^a (2933.2) ^b	CH ₃ asym
$\nu_5 + 2\nu_{39}$	2498 ^c	2898	2880	2.07	2938 ^a	
$\nu_6 + 2\nu_{39}$	2487 ^c	2887	2861	0.56	2881	
ν_3	3021	2885	2894	31.32	2881 (2880.0) ^b	CH ₃ sym
$\nu_8 + 2\nu_{39}$	2469 ^c	2880	2860	0.31		
$\nu_5 + \nu_{32}$	2961	2879	2870	0.10		
$\nu_7 + 2\nu_{39}$	2474 ^c	2871	2853	0.11		
$2\nu_{12}$	2899	2850	2847	0.08		
$\nu_{12} + \nu_{14}$	2852	2805	2799	0.24	2782 ^a	
$2\nu_{14}$	2788	2741	2707	0.63	2742	
$\nu_{11} + \nu_{21}$	2421	2396	2392	0.33		
$\nu_{14} + \nu_{21}$	2354	2338	2329	0.27		
ν_4	2370	2305	2281	8.18	2304 2299 ^a 2292 ^a 2288 ^a	CD sym (ring)
ν_5	2355	2277	2268	22.66	2281	CD asym
ν_6	2345	2266	2226	5.96	2269 2267 ^a	CD asym
ν_8	2327	2259	2233	3.38	2260	CD asym
ν_7	2331	2251	2241	1.20	2249	CD asym
$\nu_9 + 2\nu_{39}$	1767 ^c	2225	2213	0.86	2235 2224	

^aAssignment uncertain. ^bFrom ref 14. ^cThe very large difference between the harmonic and the VSCF frequency (the VSCF frequencies for ν_{39} and $2\nu_{39}$ seem overestimated), may be due to a breakdown of the VSCF separability approximation for soft torsional motions.²¹ The methyl torsional rotation mode ν_{39} may require description by angular coordinates (not by normal modes). The interpretation of this specific torsion is thus open to doubt.

(black line) show a complicated structure compared to the three theoretical fundamental transitions. They have substantial widths and a number of very narrow features. To recall, the major splitting may be caused by Fermi resonances and the coupling with librational modes and rotation of the methyl group. The fine features in the spectrum may be due to matrix-site effects.

Ne Matrix Experiment: Spectrum of $\text{C}_6\text{D}_5\text{CD}_3$ Compared to the B3LYP VSCF Calculations. The IR spectrum of fully deuterated toluene $\text{C}_6\text{D}_5\text{CD}_3$ in a Ne matrix is compared to the B3LYP VSCF calculations in Figure 7. The frequencies and intensities are listed in Table S2 (Supporting Information). The assignments for the 2136, 2221, and 2244 cm^{-1} experimental bands to the CD_3 VSCF fundamentals are indicated by dashed lines. The VSCF transitions (except the one predicted at 2304 cm^{-1}) are red-shifted compared to the experimental ones. We note that the average red shift of the VSCF for the CD_3 stretching (38 cm^{-1}) is larger than that of the aromatic CD group (<5 cm^{-1}). A similar situation arises between the CD_3 stretching modes of $\text{C}_6\text{H}_5\text{CD}_3$ (Figure 6b) and the CD stretching modes of $\text{C}_6\text{D}_5\text{CH}_3$ (Figure 5a). The red shifts of the computational frequencies compared to the

experiment are due to the weakness of the B3LYP potential. The B3LYP potentials are typically less stiff and tends to underestimate CH (or CD) bonds strength in many cases.^{3,72}

The experimental spectrum (black line) is split into many peaks compared to eight theoretical fundamentals. We propose that the major splitting (e.g., the triplet around 2220 cm^{-1}) can originate from Fermi resonances. The fine features in Figure 7 may be due to matrix site effects. The CD_3 bands in this figure are narrower than the CH_3 bands of the normal toluene in Figure 2. The fwhh value (6 cm^{-1}) of the most intense experimental peak, which was used in the previous cases for the convoluted spectrum red line, seems to be too large in this region.

It is interesting to compare the calculated and experimental deuteration effect on the CH stretching frequencies. In fact, the H/D frequency ratio changes between the harmonic and anharmonic calculations. For the ν_2 mode of $\text{C}_6\text{H}_5\text{CH}_3$ and $\text{C}_6\text{D}_5\text{CD}_3$, this ratio is 1.351 in the harmonic approximation and 1.325 in the VSCF calculation. The anharmonic VSCF value is in an excellent agreement with the experiment (1.330).

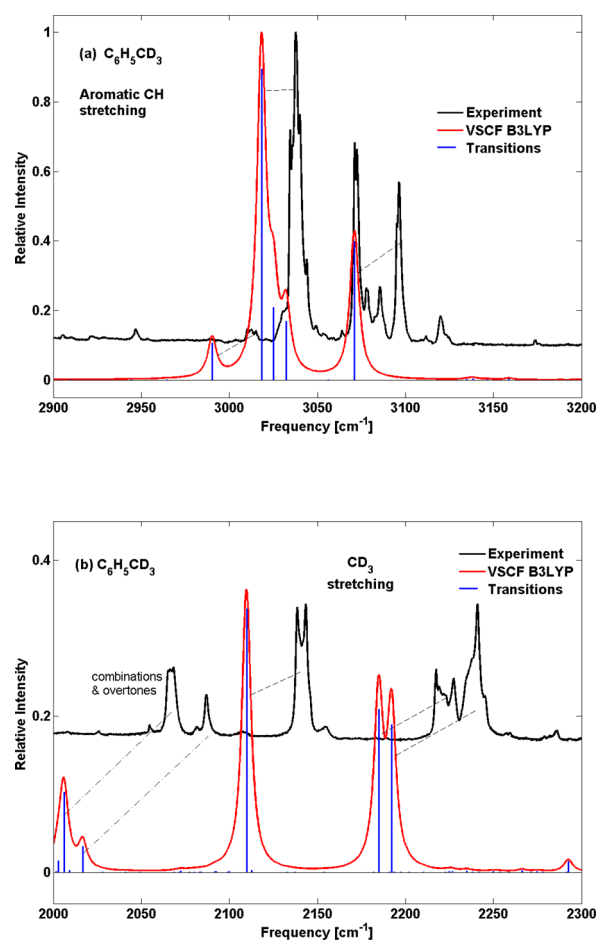


Figure 6. B3LYP VSCF spectra of partially deuterated toluene $C_6H_5CD_3$ with combinations and overtones (red line) and VSCF lines corresponding to all the transitions in this spectral range (blue lines) compared to the Ne matrix experiment (black line). (a) Aromatic CH stretching region. (b) CD_3 stretching region.

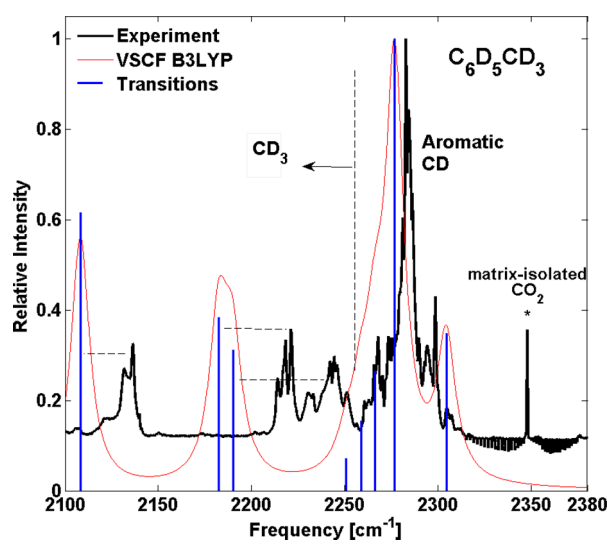


Figure 7. B3LYP VSCF spectrum of fully deuterated toluene $C_6D_5CD_3$ (red line) and VSCF lines corresponding to all fundamental transitions in this spectral range (blue lines) compared to the Ne matrix experiment (black line).

CONCLUDING REMARKS

In the present work, we compared the anharmonic B3LYP VSCF calculations for isolated toluene with the experiments on toluene in a Ne matrix and in the liquid phase. A number of toluene isotopologues were comparatively studied to support the assignments.

The B3LYP VSCF theory seems to be successful in providing a good agreement with the experiment for the main CH stretching bands. This success is due to the treatment of the vibrations of an isolated molecule, using a reliable anharmonic potential energy surface (B3LYP/cc-pVDZ), with first-principles calculations. The treatment of anharmonic vibrations in this method is an advantage due to their major importance for this system. The harmonic CH stretching frequencies are much inferior in accuracy to the VSCF ones for a given potential and basis set.

In a Ne matrix, numerous peaks are seen that are not predicted by the calculations. The major band splittings may originate from Fermi resonances, which is supported by previous research.¹¹ The calculations of the overtone and combination transitions near the fundamental frequencies indicate the possibility of such Fermi resonances. The fine band splittings in the Ne matrix spectrum can originate from different matrix sites.

In both liquid-phase (at 298 K) and Ne-matrix spectra (at 3 K) of toluene, the main peak has a fwhm of about 6 cm^{-1} (the other peaks in the liquid phase are broader, as shown in Figure 4). This observation is surprising because the temperature difference between these two experiments is huge. We think that a source of the broadening can be due to fast intramolecular vibrational energy redistribution, which is not included into the present theory. This mechanism entails transfer of energy from a fundamental transition to other vibrational degrees of freedom, which, therefore, reduces the lifetime of the excited state and gives rise to a corresponding width by the uncertainty principle. This mechanism is expected to be insensitive to the temperature and to the coupling with the matrix, because the energy flow is intramolecular; hence, it can operate even at 3 K. However, there are other broadening mechanisms, which are different in these two media. In the liquid phase, it is collisional (homogeneous) broadening. In a low-temperature matrix, the fine splitting of the bands is probably due to a variation of the local morphology (matrix-site effect) leading to inhomogeneous broadening.

Additional mechanisms are possible for the broadening and splitting of the lines. For example, couplings of the fundamental modes with librational motions and rotation of the methyl group are also possible. It should be also emphasized that we did not calculate all possible combinations modes and overtones, and these transitions can complicate the spectrum.

In summary, the state-of-the-art anharmonic calculations for toluene in vacuum are proven to be successful in providing interpretation for most of the observed spectroscopic features in two very different environments. Several deviations and unexplained features remain, especially for the Ne matrix experiments. Spectroscopic treatment that includes environmental effects requires much further progress and is left for the future.

■ ASSOCIATED CONTENT

■ Supporting Information

The Supporting Information is available free of charge on the ACS Publications website at DOI: 10.1021/acs.jpca.6b01604.

Ne matrix experimental spectra and B3LYP VSCF calculations of $C_6H_5CD_3$ (Table S1) and $C_6D_5CD_3$ (Table S2) (PDF)

■ AUTHOR INFORMATION

Corresponding Author

*R. Benny Gerber. E-mail: benny@fh.huji.ac.il. Tel: +972-2-6585732.

Notes

The authors declare no competing financial interest.

■ ACKNOWLEDGMENTS

Research at the Hebrew University was supported under the auspices of the Saerree K. and Louis P. Fiedler Chair in chemistry (R.B.G.). The research at the University of Helsinki was supported by the Academy of Finland through the FiDiPro program and grants No. 1139105 and No. 1277993. E.O.P acknowledges support from the National Science Foundation, Grant No. CHE-1414466.

■ REFERENCES

- (1) Chung, C.-Y.; Boik, J.; Potma, E. O. Biomolecular Imaging with Coherent Nonlinear Vibrational Microscopy. *Annu. Rev. Phys. Chem.* **2013**, *64*, 77–99.
- (2) Šebek, J.; Pele, L.; Potma, E. O.; Gerber, R. B. Raman Spectra of Long Chain Hydrocarbons: Anharmonic Calculations, Experiment and Implications for Imaging of Biomembranes. *Phys. Chem. Chem. Phys.* **2011**, *13*, 12724–12733.
- (3) Šebek, J.; Knaanie, R.; Albee, B.; Potma, E. O.; Gerber, R. B. Spectroscopy of the C-H Stretching Vibrational Band in Selected Organic Molecules. *J. Phys. Chem. A* **2013**, *117*, 7442–7452.
- (4) Bertie, J. E.; Jones, R. N.; Apelblat, Y.; Keefe, C. D. Infrared Intensities of Liquids XIII: Accurate Optical-Constants and Molar Absorption-Coefficients between 6500 and 435 cm^{-1} of Toluene at 25 °C, from Spectra Recorded in Several Laboratories. *Appl. Spectrosc.* **1994**, *48*, 127–143.
- (5) Bertie, J. E.; Apelblat, Y.; Keefe, C. D. Infrared Intensities of Liquids XXV: Dielectric Constants, Molar Polarizabilities and Integrated Intensities of Liquid Toluene at 25 °C between 4800 and 400 cm^{-1} . *J. Mol. Struct.* **2005**, *750*, 78–93.
- (6) Keefe, C. D.; MacDonald, J. L. Vibrational Assignment, Integrated Intensities of Liquid Toluene- d_8 from 4000 to 450 cm^{-1} at 25 °C. *Spectrochim. Acta, Part A* **2006**, *64*, 483–494.
- (7) Baker, J. A Scaled Quantum Mechanical Reinvestigation of the Vibrational Spectrum of Toluene. *J. Mol. Struct.: THEOCHEM* **2008**, *865*, 49–52.
- (8) Hitchcock, A. P.; Laposa, J. D. Vibrational Frequencies of Toluene- d_5 . *J. Mol. Spectrosc.* **1975**, *54*, 223–230.
- (9) Selco, J. I.; Carrick, P. G. Jet Cooled Emission-Spectra of Toluene and the Benzyl Radical. *J. Mol. Spectrosc.* **1989**, *137*, 13–23.
- (10) Hickman, C. G.; Gascooke, J. R.; Lawrance, W. D. The $S_1-S_0(^1B_2-^1A_1)$ Transition of Jet-Cooled Toluene: Excitation and Dispersed Fluorescence Spectra, Fluorescence Lifetimes, and Intramolecular Vibrational Energy Redistribution. *J. Chem. Phys.* **1996**, *104*, 4887–4901.
- (11) Minejima, C.; Ebata, T.; Mikami, N. C–H Stretching Vibrations of Benzene and Toluene in Their S_1 States Observed by Double Resonance Vibrational Spectroscopy in Supersonic Jets. *Phys. Chem. Chem. Phys.* **2002**, *4*, 1537–1541.
- (12) *Physics and Chemistry at Low Temperatures*; Khriachtchev, L., Ed.; Pan Stanford Publishing: Singapore, 2011.
- (13) Cao, Q.; Andrijchenko, N.; Ermilov, A.; Räsänen, M.; Nemukhin, A.; Khriachtchev, L. Interaction of Aromatic Compounds with Xenon: Spectroscopic and Computational Characterization for the Cases of *p*-Cresol and Toluene. *J. Phys. Chem. A* **2015**, *119*, 2587–2593.
- (14) Cao, Q.; Gor, G. Y.; Krogh-Jespersen, K.; Khriachtchev, L. Non-Covalent Interactions of Nitrous Oxide with Aromatic Compounds: Spectroscopic and Computational Evidence for the Formation of 1:1 Complexes. *J. Chem. Phys.* **2014**, *140*, 144304.
- (15) Pratt, D. W. High Resolution Spectroscopy in the Gas Phase: Even Large Molecules Have Well-Defined Shapes. *Annu. Rev. Phys. Chem.* **1998**, *49*, 481–530.
- (16) Gerber, R. B.; Chaban, G. M.; Brauer, B.; Miller, Y. *Theory and Applications of Computational Chemistry: The First 40 Years*; 2005; Chapter 9, pp 165–193.
- (17) Brauer, B.; Gerber, R. B.; Kabeláč, M.; Hobza, P.; Bakker, J. M.; Riziq, A. G. A.; de Vries, M. S. Vibrational Spectroscopy of the G··C Base Pair: Experiment, Harmonic and Anharmonic Calculations, and the Nature of the Anharmonic Couplings. *J. Phys. Chem. A* **2005**, *109*, 6974–6984.
- (18) Chaban, G. M.; Jung, J. O.; Gerber, R. B. Anharmonic Vibrational Spectroscopy of Glycine: Testing of ab Initio and Empirical Potentials. *J. Phys. Chem. A* **2000**, *104*, 10035–10044.
- (19) Bowman, J. M. The Self-Consistent-Field Approach to Polyatomic Vibrations. *Acc. Chem. Res.* **1986**, *19*, 202–208.
- (20) Pele, L.; Šebek, J.; Potma, E. O.; Gerber, R. B. Raman and IR Spectra of Butane: Anharmonic Calculations and Interpretation of Room Temperature Spectra. *Chem. Phys. Lett.* **2011**, *515*, 7–12.
- (21) Roy, T. K.; Gerber, R. B. Vibrational Self-Consistent Field Calculations for Spectroscopy of Biological Molecules: New Algorithmic Developments and Applications. *Phys. Chem. Chem. Phys.* **2013**, *15*, 9468–9492.
- (22) Barone, V. Anharmonic Vibrational Properties by a Fully Automated Second-Order Perturbative Approach. *J. Chem. Phys.* **2005**, *122*, 014108.
- (23) Barone, V.; Biczysko, M.; Bloino, J. Fully Anharmonic IR and Raman Spectra of Medium-Size Molecular Systems: Accuracy and Interpretation. *Phys. Chem. Chem. Phys.* **2014**, *16*, 1759–1787.
- (24) Frisch, M. J.; Trucks, G. W.; Schlegel, H. B.; et al. GAUSSIAN03, revision C.01; Gaussian, Inc.: Pittsburgh, PA, 2003.
- (25) Gaigeot, M. P. Theoretical Spectroscopy of Floppy Peptides at Room Temperature. A DFTMD Perspective: Gas and Aqueous Phase. *Phys. Chem. Chem. Phys.* **2010**, *12*, 3336–3359.
- (26) Gaigeot, M. P.; Sprik, M. Ab Initio Molecular Dynamics Computation of the Infrared Spectrum of Aqueous Uracil. *J. Phys. Chem. B* **2003**, *107*, 10344–10358.
- (27) Cimas, A.; Vaden, T. D.; de Boer, T.; Snoek, L. C.; Gaigeot, M. P. Vibrational Spectra of Small Protonated Peptides from Finite Temperature MD Simulations and IRMPD Spectroscopy. *J. Chem. Theory Comput.* **2009**, *5*, 1068–1078.
- (28) Gregoire, G.; Gaigeot, M. P.; Marinica, D. C.; Lemaire, J.; Schermann, J. P.; Desfrancois, C. Resonant Infrared Multiphoton Dissociation Spectroscopy of Gas-Phase Protonated Peptides. Experiments and Car-Parrinello Dynamics at 300 K. *Phys. Chem. Chem. Phys.* **2007**, *9*, 3082–3097.
- (29) Car, R.; Parrinello, M. Unified Approach for Molecular-Dynamics and Density-Functional Theory. *Phys. Rev. Lett.* **1985**, *55*, 2471–2474.
- (30) Bowman, J. M.; Christoffel, K.; Tobin, F. Application of SCF-SI Theory to Vibrational Motion in Polyatomic Molecules. *J. Phys. Chem.* **1979**, *83*, 905–912.
- (31) Ratner, M. A.; Buch, V.; Gerber, R. B. The Semiclassical Self-Consistent-Field (SC-SCF) Approach to Energy Levels of Coupled Vibrational Modes. II. The Semiclassical State-Interaction Procedure. *Chem. Phys.* **1980**, *53*, 345–356.
- (32) Wang, X.-G.; Carrington, T. Six-Dimensional Variational Calculation of the Bending Energy Levels of HF Trimer and DF Trimer. *J. Chem. Phys.* **2001**, *115*, 9781–9796.

- (33) Avila, G.; Carrington, T. Solving the Vibrational Schrödinger Equation Using Bases Pruned to Include Strongly Coupled Functions and Compatible Quadratures. *J. Chem. Phys.* **2012**, *137*, 174108.
- (34) Scott, A. P.; Radom, L. Harmonic Vibrational Frequencies: An Evaluation of Hartree–Fock, Møller–Plesset, Quadratic Configuration Interaction, Density Functional Theory and Semiempirical Scale Factors. *J. Phys. Chem.* **1996**, *100*, 16502–16513.
- (35) Sinha, P.; Boesch, S. E.; Gu, C. M.; Wheeler, R. A.; Wilson, A. K. Harmonic Vibrational Frequencies: Scaling Factors for HF, B3LYP, and MP2 Methods in Combination with Correlation Consistent Basis Sets. *J. Phys. Chem. A* **2004**, *108*, 9213–9217.
- (36) Schmidt, M. W.; et al. General Atomic and Molecular Electronic-Structure System. *J. Comput. Chem.* **1993**, *14*, 1347–1363.
- (37) Pele, L.; Gerber, R. B. On the Number of Significant Mode-Mode Anharmonic Couplings in Vibrational Calculations: Correlation-Corrected Vibrational Self-Consistent Field Treatment of Di-, Tri-, and Tetrapeptides. *J. Chem. Phys.* **2008**, *128*, 165105.
- (38) Brauer, B.; Pincu, M.; Buch, V.; Bar, I.; Simons, J. P.; Gerber, R. B. Vibrational Spectra of α -Glucose, β -Glucose, and Sucrose: Anharmonic Calculations and Experiment. *J. Phys. Chem. A* **2011**, *115*, 5859–5872.
- (39) Becke, A. D. Density-Functional Exchange-Energy Approximation with Correct Asymptotic Behavior. *Phys. Rev. A: At, Mol., Opt. Phys.* **1988**, *38*, 3098–3100.
- (40) Becke, A. D. Density-Functional Thermochemistry. III. The Role of Exact Exchange. *J. Chem. Phys.* **1993**, *98*, 5648–5652.
- (41) Møller, C.; Plesset, M. S. Note on an Approximation Treatment for Many-Electron Systems. *Phys. Rev.* **1934**, *46*, 618–622.
- (42) Dunning, T. H., Jr. Gaussian Basis Sets for Use in Correlated Molecular Calculations. I. The Atoms Boron through Neon and Hydrogen. *J. Chem. Phys.* **1989**, *90*, 1007–1023.
- (43) Kendall, R. A.; Dunning, T. H., Jr.; Harrison, R. J. Electron Affinities of the First-Row Atoms Revisited. Systematic Basis Sets and Wave Functions. *J. Chem. Phys.* **1992**, *96*, 6796–6806.
- (44) Chaban, G. M.; Gerber, R. B. Anharmonic Vibrational Spectroscopy Calculations with Electronic Structure Potentials: Comparison of MP2 and DFT for Organic Molecules. *Theor. Chem. Acc.* **2008**, *120*, 273–279.
- (45) Knaanie, R.; Sebek, J.; Kalinowski, J.; Benny Gerber, R. Hybrid MP2/MP4 Potential Surfaces in VSCF Calculations of IR Spectra: Applications for Organic Molecules. *Spectrochim. Acta, Part A* **2014**, *119*, 2–11.
- (46) Bowman, J. M. Self-Consistent Field Energies and Wavefunctions for Coupled Oscillators. *J. Chem. Phys.* **1978**, *68*, 608–610.
- (47) Gerber, R. B.; Ratner, M. A. Semi-Classical Self-Consistent Field (SC SCF) Approximation for Eigenvalues of Coupled-Vibration Systems. *Chem. Phys. Lett.* **1979**, *68*, 195–198.
- (48) Gerber, R. B.; Ratner, M. A. Self-Consistent-Field Methods for Vibrational Excitations in Polyatomic Systems. *Adv. Chem. Phys.* **1988**, *70*, 97–132.
- (49) Gregurick, S. K.; Fredj, E.; Elber, R.; Gerber, R. B. Vibrational Spectroscopy of Peptides and Peptide-Water Complexes: Anharmonic Coupled-Mode Calculations. *J. Phys. Chem. B* **1997**, *101*, 8595–8606.
- (50) Gregurick, S. K.; Liu, J. H.-Y.; Brant, D. A.; Gerber, R. B. Anharmonic Vibrational Self-Consistent Field Calculations as an Approach to Improving Force Fields for Monosaccharides. *J. Phys. Chem. B* **1999**, *103*, 3476–3488.
- (51) Gerber, R. B.; Brauer, B.; Gregurick, S. K.; Chaban, G. M. Calculation of Anharmonic Vibrational Spectroscopy of Small Biological Molecules. *PhysChemComm* **2002**, *5*, 142–150.
- (52) Neugebauer, J.; Hess, B. A. Fundamental Vibrational Frequencies of Small Polyatomic Molecules from Density-Functional Calculations and Vibrational Perturbation Theory. *J. Chem. Phys.* **2003**, *118*, 7215–7225.
- (53) Espinoza, C.; Szczepanski, J.; Vala, M.; Polfer, N. C. Glycine and Its Hydrated Complexes: A Matrix Isolation Infrared Study. *J. Phys. Chem. A* **2010**, *114*, 5919–5927.
- (54) Seidler, P.; Kaga, T.; Yagi, K.; Christiansen, O.; Hirao, K. On the Coupling Strength in Potential Energy Surfaces for Vibrational Calculations. *Chem. Phys. Lett.* **2009**, *483*, 138–142.
- (55) Christiansen, O.; Luis, J. M. Beyond Vibrational Self-Consistent-Field Methods: Benchmark Calculations for the Fundamental Vibrations of Ethylene. *Int. J. Quantum Chem.* **2005**, *104*, 667–680.
- (56) Chaban, G. M.; Gerber, R. B. Anharmonic Vibrational Spectroscopy of the Glycine–Water Complex: Calculations for Ab Initio, Empirical, and Hybrid Quantum Mechanics/Molecular Mechanics Potentials. *J. Chem. Phys.* **2001**, *115*, 1340–1348.
- (57) Carter, S.; Culik, S. J.; Bowman, J. M. Vibrational Self-Consistent Field Method for Many-Mode Systems: A New Approach and Application to the Vibrations of Co Adsorbed on Cu(100). *J. Chem. Phys.* **1997**, *107*, 10458–10469.
- (58) Chaban, G. M.; Jung, J. O.; Gerber, R. B. Ab Initio Calculation of Anharmonic Vibrational States of Polyatomic Systems: Electronic Structure Combined with Vibrational Self-Consistent Field. *J. Chem. Phys.* **1999**, *111*, 1823–1829.
- (59) Jung, J. O.; Gerber, R. B. Vibrational Wave Functions and Spectroscopy of $(\text{H}_2\text{O})_n$, $n=2,3,4,5$: Vibrational Self-Consistent Field with Correlation Corrections. *J. Chem. Phys.* **1996**, *105*, 10332–10348.
- (60) Norris, L. S.; Ratner, M. A.; Roitberg, A. E.; Gerber, R. B. Møller-Plesset Perturbation Theory Applied to Vibrational Problems. *J. Chem. Phys.* **1996**, *105*, 11261–11267.
- (61) Pele, L.; Brauer, B.; Gerber, R. B. Acceleration of Correlation-Corrected Vibrational Self-Consistent Field Calculation Times for Large Polyatomic Molecules. *Theor. Chem. Acc.* **2007**, *117*, 69–72.
- (62) Benoit, D. M. Efficient Correlation-Corrected Vibrational Self-Consistent Field Computation of OH-Stretch Frequencies Using a Low-Scaling Algorithm. *J. Chem. Phys.* **2006**, *125*, 244110–244111.
- (63) Christiansen, O. Møller-Plesset Perturbation Theory for Vibrational Wave Functions. *J. Chem. Phys.* **2003**, *119*, 5773–5781.
- (64) Bowman, J. M.; Carter, S.; Huang, X. Multimode: A Code to Calculate Rovibrational Energies of Polyatomic Molecules. *Int. Rev. Phys. Chem.* **2003**, *22*, 533–549.
- (65) Rauhut, G. Efficient Calculation of Potential Energy Surfaces for the Generation of Vibrational Wave Functions. *J. Chem. Phys.* **2004**, *121*, 9313–9322.
- (66) Scribano, Y.; Benoit, D. M. Calculation of Vibrational Frequencies through a Variational Reduced-Coupling Approach. *J. Chem. Phys.* **2007**, *127*, 164118.
- (67) Yagi, K.; Hirata, S.; Hirao, K. Vibrational Quasi-Degenerate Perturbation Theory: Applications to Fermi Resonance in CO_2 , H_2CO , and C_6H_6 . *Phys. Chem. Chem. Phys.* **2008**, *10*, 1781–1788.
- (68) Roy, T. K.; Prasad, M. D. Development of a New Variational Approach for Thermal Density Matrices. *J. Chem. Phys.* **2011**, *134*, 214110.
- (69) Matsunaga, N.; Chaban, G. M.; Gerber, R. B. Degenerate Perturbation Theory Corrections for the Vibrational Self-Consistent Field Approximation: Method and Applications. *J. Chem. Phys.* **2002**, *117*, 3541–3547.
- (70) Daněček, P.; Bouř, P. Comparison of the Numerical Stability of Methods for Anharmonic Calculations of Vibrational Molecular Energies. *J. Comput. Chem.* **2007**, *28*, 1617–1624.
- (71) Njegic, B.; Gordon, M. S. Exploring the Effect of Anharmonicity of Molecular Vibrations on Thermodynamic Properties. *J. Chem. Phys.* **2006**, *125*, 224102.
- (72) Roy, T. K.; Carrington, T.; Gerber, R. B. Approximate First-Principles Anharmonic Calculations of Polyatomic Spectra Using MP2 and B3LYP Potentials: Comparisons with Experiment. *J. Phys. Chem. A* **2014**, *118*, 6730–6739.